Inorganic Chemistry

Article

pubs.acs.org/IC

Tiara-like Octanuclear Palladium(II) and Platinum(II) Thiolates and Their Inclusion Complexes with Dihalo- or Iodoalkanes

Yukari Yamashina, Yasutaka Kataoka, and Yasuyuki Ura*

Department of Chemistry, Faculty of Science, Nara Women's University, Kitauoyanishi-machi, Nara 630-8506, Japan

Supporting Information

ABSTRACT: A tiara-like octanuclear palladium thiolate complex, $[Pd(\mu\text{-}SCH_2CO_2Me)_2]_8$, that has a toroidal structure was synthesized via reactions of either $PdCl_2$ with methyl thioglycolate/*N*,*N*-diisopropylethylamine (DIEA) (conventional method) or $[PdCl_2(MeCN)_2]$ with *m*-$C_6H_4(CMe_2SCH_2CO_2Me)_2$ (alternative method). In the latter method, the tiara-like complex formed via the corresponding SCS-pincer complex and/or 1:1 $PdCl_2$ and ligand complexes. With respect to the platinum analogues, the alternative method efficiently produced the tiara-like octanuclear complex $[Pt(\mu\text{-}SCH_2CO_2Me)_2]_8$ in high purity. Small molecules, such as CH_2Cl_2, $ClCH_2CH_2Cl$, CH_2Br_2, and CH_3I, were accommodated in the inner voids of the tiara rings to form 1:1 inclusion complexes. These complexes are stabilized not only by weak CH···X hydrogen bonds (X = Cl or Br) between the methylene protons of four or eight axially positioned methoxycarbonylmethyl groups on the tiara rings and the halogen atoms of the guest molecules but also by weak coordination of the halogen atoms to the transition-metal atoms.

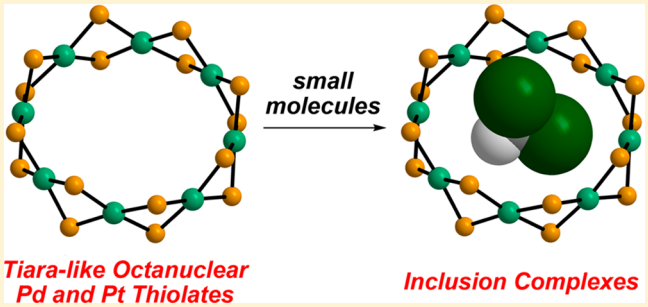

INTRODUCTION

Metal thiolates are an important class of compounds because of their structural diversity in coordination chemistry,[1−3] relevance to cofactors of metalloproteins in biological systems,[4,5] and importance in cluster and surface science[6,7] and catalysis.[8] Thiolate-bridged polynuclear group 10 transition-metal complexes with chain structures that have the general formula of $[M(\mu\text{-}SR)_2]_n$ (M = Ni, Pd) have been investigated in detail because they provide efficient catalysis of atom-economical organic reactions such as regioselective additions of thiols and disulfides across alkynes.[8−13] Tiara-like complexes, which are also polynuclear group 10 transition-metal thiolates and are characterized by toroidal architectures, have been studied extensively, both in terms of their intriguing structural features and with respect to the preparation of monodisperse metal sulfide nanoparticles,[14] nonlinear optical materials,[15] photoactive water-reducing catalysts,[16,17] and host−guest chemistry.[15,18−21] Tiara-like nickel complexes have received considerable attention, resulting in the preparation of complexes with a variety of ring sizes that have the general formula of $[Ni(\mu\text{-}SR)_2]_n$ (n = 4−6, 8−12).[15,17,18,20−35] In contrast, although several tiara-like hexanuclear palladium complexes have been reported,[9,14,19,36−43] only one octanuclear complex, namely, $[Pd(\mu\text{-}S^nPr)_2]_8$, is known and was obtained as a mixture with hexanuclear $[Pd(\mu\text{-}S^nPr)_2]_6$.[19] For platinum, infinite thiolates and selenolates that have the general formula of $[Pt(\mu\text{-}ER)_2]_\infty$ (E = S, Se) have been synthesized using a solvothermal method;[37] however, to the best of our knowledge, no tiara-like complexes have been reported thus far.

In most cases, tiara-like nickel and palladium complexes are synthesized through the reactions of group 10 transition-metal halides with thiols in the presence or absence of a base. We successfully synthesized an octanuclear palladium complex using this conventional method. Moreover, we also developed an alternative synthetic method using *m*-$C_6H_4(CMe_2SR)_2$ as the thiolate ligand source. The latter method was found to be advantageous for the synthesis of a platinum complex. In this paper, we report not only the synthesis, using these two methods, of novel tiara-like octanuclear palladium and platinum complexes but also the inclusion complexes with small organic molecules. Decanuclear and undecanuclear nickel complexes have been reported to include solvent molecules, such as benzene,[20] toluene,[15] and tetrahydrofuran (THF),[21] in their inner voids. In contrast, no tiara-like palladium inclusion complexes have been reported thus far.

RESULTS AND DISCUSSION

Synthesis and Structure of Tiara-like Octanuclear Palladium Complex 1. $PdCl_2$ was reacted with 2 equiv each of methyl thioglycolate and *N*,*N*-diisopropylethylamine (DIEA) in ^{n}PrOH at room temperature. After 4 h, a tiara-like octanuclear complex, that is, $[Pd(\mu\text{-}SCH_2CO_2Me)_2]_8$ (**1**), was obtained in high isolated yield (90%) (Scheme 1); a high concentration of palladium (0.25 M) is essential to achieve a high yield because a lower concentration (0.04 M) resulted in lower yield (67%). The molecular structure of complex **1** was

Received: December 12, 2013
Published: March 24, 2014

   dx.doi.org/10.1021/ic403050c | Inorg. Chem. 2014, 53, 3558−3567

Scheme 1. Formation of Tiara-like Octanuclear Palladium Complex 1

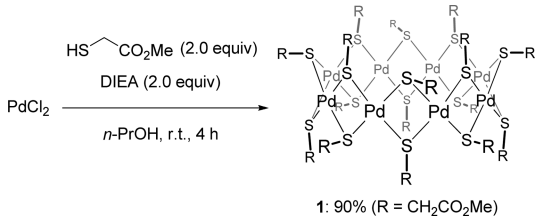

determined by X-ray crystallography (Figure 1, recrystallized from $CHCl_3$/hexane). The eight palladium atoms lie on a nearly planar surface and form an octagonal structure with the distances between two adjacent metal atoms ranging from 3.1398(9) to 3.2745(10) Å; the average Pd···Pd distance is 3.23(4) Å, which is slightly longer than the metal−metal distances in $[Pd(\mu\text{-}S^nPr)_2]_8$ (3.17 Å)[19] and an octanuclear nickel analog, $[Ni(\mu\text{-}SCH_2CO_2Et)_2]_8$ (3.05 Å).[18] Each palladium atom is coordinated by four μ_2-bridged thiolate ligands and has an almost square planar geometry. The Pd−S bond distances are within 2.305(2)−2.367(4) Å (average: 2.32(2) Å). The horizontal and vertical S−Pd−S bond angles vary between 93.50(14) and 99.21(8)° (average: 97.3(14)°) and 81.65(8) and 85.35(14)° (average: 83.0(9)°), respectively. The Pd−S−Pd bond angles are within 85.20(8)−91.70(17)° (average: 88.4(16)°), and the dihedral angles between the PdS_4 planes are within 127.75(6)−138.41(6)° (average: 135(4)°). The distances between two adjacent sulfur atoms in the two S_8 rings are within the range of 3.336(6)−3.573(6) Å (average: 3.48(5) Å). The 16 methoxycarbonylmethyl arms are alternately located at axial and equatorial positions (i.e., the arms extend nearly perpendicularly and horizontally from the tiara ring), and some are significantly disordered; in particular, the axial arm on the S1 atom alternates between bending inward to occupy the inner void and extending out of the toroidal structure (~1:1). A similar inward curvature of an arm was also observed in $[Ni(\mu\text{-}SCH_2CO_2Et)_2]_8$.[18] The axial arm on the S2 atom, which is located trans to S1 on the other rim of the tiara, closes the lid from the bottom. The distances between the diagonally positioned palladium atoms are Pd1···Pd5 = 8.7191(9) Å, Pd2···Pd6 = 8.2331(9) Å, Pd3···Pd7 = 8.2307(8) Å, and Pd4···Pd8 = 8.5895(8) Å, resulting in an ellipsoidal architecture of the tiara ring (average: 8.44 Å). These distances are considerably longer than those of $[Ni(\mu\text{-}SCH_2CO_2Et)_2]_8$ (7.59−8.34 Å, average: 7.95 Å).[18]

The above-mentioned geometrical parameters for **1** were compared with those of the previously reported hexanuclear palladium complexes $[Pd(\mu\text{-}SCH_2CO_2Me)_2]_6$[39] and $[Pd(\mu\text{-}S^nHex)_2]_6$.[9] The average distance between the two adjacent palladium atoms in the hexanuclear complexes is 3.11 Å, which is approximately 0.1 Å shorter than that in **1**. Although the

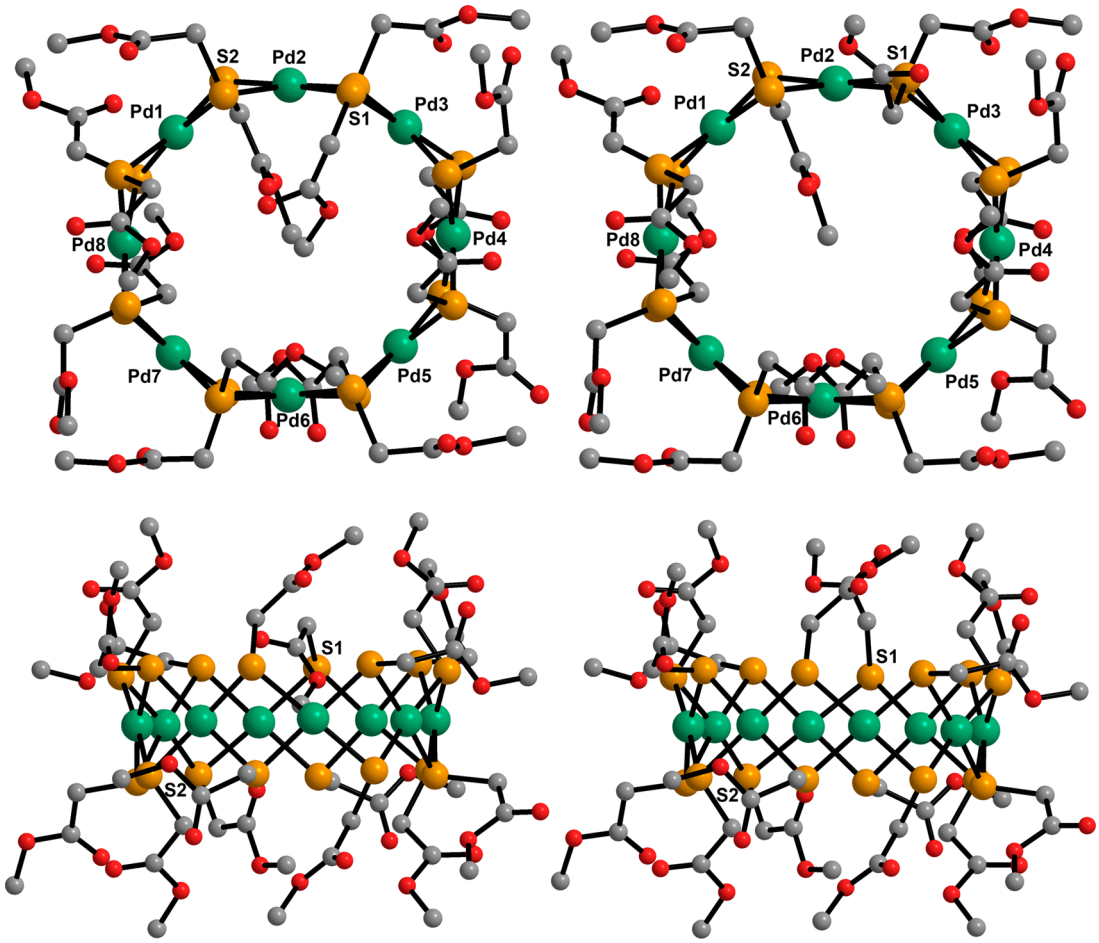

Figure 1. Molecular structure of complex **1** with an inwardly bent arm (left) and outwardly stretched arm (right) on S1 atom. (upper) Top view. (lower) Side view. Hydrogen atoms are omitted for clarity. Pd: light green, S: orange, C: gray, O: red.

dx.doi.org/10.1021/ic403050c | Inorg. Chem. 2014, 53, 3558−3567

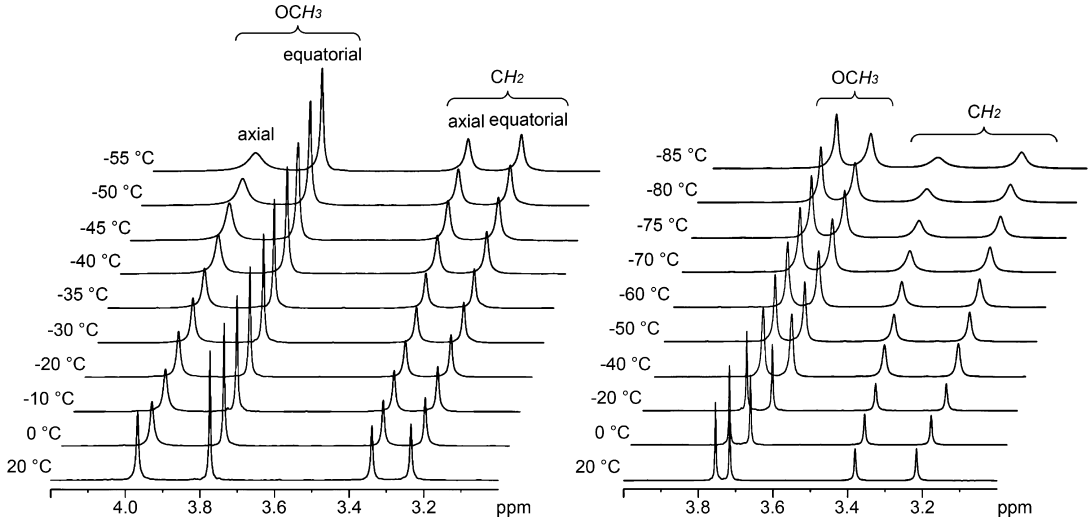

Figure 2. Variable-temperature ^{1}H NMR spectra (400 MHz) of **1** in (left) $CDCl_3$, −55−20 °C and (right) CD_2Cl_2, −85−20 °C.

averages of the horizontal and vertical S−Pd−S bond angles are similar for these three complexes (97.8(5)° and 82.4(5)° for $[Pd(\mu\text{-}SCH_2CO_2Me)_2]_6$; 98.0(5)° and 81.9(5)° for $[Pd(\mu\text{-}S^nHex)_2]_6$), the average Pd−S−Pd bond angle for the hexanuclear complexes is 84.5°, which is approximately 4° smaller than that found for **1**. The dihedral angles between the PdS_4 planes are also small: 113.47(3)−124.36(4)° for $[Pd(\mu\text{-}SCH_2CO_2Me)_2]_6$ and 115.19(6)−126.53(7)° for $[Pd(\mu\text{-}S^nHex)_2]_6$. The distances between the diagonally positioned palladium atoms in $[Pd(\mu\text{-}S^nHex)_2]_6$ are within 6.053−6.461 Å. The average distance (6.23 Å) is approximately 2.2 Å shorter than that in **1**.

The matrix-assisted laser desorption ionization time-of-flight mass spectrometry (MALDI-TOF MS) spectrum of **1** revealed a parent peak at m/z 2556.3 (with Na^+, calcd 2556.2) and a small fragment peak at m/z 2240.4 assignable to $[Pd(\mu\text{-}SCH_2CO_2Me)_2]_7$ (with Na^+, calcd 2238.3) (Figures S1−S3 in Supporting Information). The ^{1}H NMR spectrum of **1** (in $CDCl_3$) features two methylene signals at 3.34 and 3.23 ppm and two methoxy signals at 3.97 and 3.77 ppm; these two sets of signals are attributed to the axial and equatorial methoxycarbonylmethyl arms, and therefore, the molecular symmetry of **1** in solution is pseudo-D_{4d}. Such separated NMR signals of axial and equatorial arms have also been observed in hexanuclear palladium complexes.[9,14,19,41,42] In contrast with $[Pd(\mu\text{-}S^nPr)_2]_8$, which exists in equilibrium with the corresponding hexanuclear complex $[Pd(\mu\text{-}S^nPr)_2]_6$,[19] **1** was stable in solution (CD_3CN) even at 70 °C, and no hexanuclear or other polynuclear complexes were observed at all. The ^{1}H NMR spectra of **1** in $CDCl_3$ and CD_2Cl_2 obtained through low-temperature measurements are shown in Figure 2. In $CDCl_3$, one of the two methoxy signals appears at 3.97 ppm as a slightly broad singlet, which is broadened further than the other signal at 3.77 ppm, upon decreasing the temperature. On the other hand, in CD_2Cl_2, both methoxy signals broaden simultaneously. This difference can be attributed to the fact that $CDCl_3$ cannot be accommodated in the inner void of **1** but CD_2Cl_2 can (vide infra). Instead of the solvent molecule, one of the axial methoxycarbonylmethyl groups can occupy the inner void in $CDCl_3$, as already shown in Figure 1. The selective peak broadening observed in the variable-temperature NMR spectra in $CDCl_3$ results from the dynamic behavior of the axial arms moving into and out of the tiara ring. Therefore, the singlet that appears at 3.97 ppm is assigned to the methoxy groups in the axial arms, and that at 3.77 ppm is attributed to the methoxy groups in the equatorial arms. Because carbonyl carbons (170.4 and 169.8 ppm) have correlations with the axial methoxy protons (3.97 ppm) and methylene protons (3.34 ppm), as well as the equatorial methoxy protons (3.77 ppm) and other methylene protons (3.23 ppm) in the heteronuclear multiple-bond correlation (HMBC) spectrum measured in $CDCl_3$, respectively, the singlet at 3.34 ppm is assigned to the methylene protons in the axial arms, and the other, at 3.23 ppm, is assigned to the methylene protons in the equatorial arms.

Alternative Synthesis of 1. Although the conventional method was successful, complex **1** could also be prepared using dimethyl [1,3-phenylenebis(1-methylethylidenethio)]diacetate (**2**) as a thiolate-ligand source in the absence of a base. $[PdCl_2(MeCN)_2]$ was reacted with 1 equiv of **2** in MeOH (0.3 M) at 70 °C (bath temperature). After 10 h, complex **1** was obtained in high yield (Scheme 2).

Scheme 2. Alternative Synthesis of 1

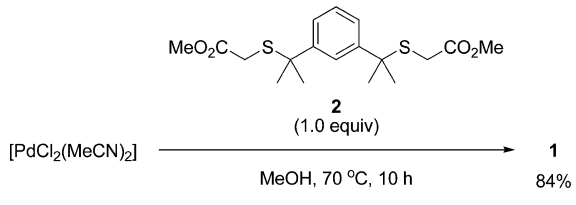

To investigate the reaction mechanism, $[PdCl_2(MeCN)_2]$ was reacted with **2** in $CHCl_3$ (0.04 M) at room temperature. After 1 h, SCS-pincer complex **3** formed selectively with 83% isolated yield; **1** was not formed at this stage (Scheme 3). After isolation, **3** was heated in CD_3CN (0.3 M) at 90 °C (bath temperature) in the presence of 1 equiv of HCl, resulting in the formation of **1** in moderate yield along with a small amount of 1,3-diisopropenylbenzene (**4**). These reactions clearly demonstrate that tiara-like complex **1** can form via SCS-pincer complex **3**. In contrast, when dimethyl[1,3-phenylenebis(methylenethio)]diacetate (**5**), which does not contain methyl groups at the benzylic positions, was used instead of **2**, higher temperatures and longer reaction times were required to

dx.doi.org/10.1021/ic403050c | Inorg. Chem. 2014, 53, 3558−3567

Scheme 3. Formation of Tiara-like Complex 1 via SCS-Pincer Complex 3

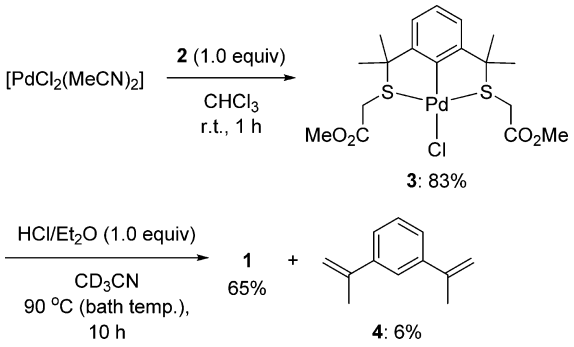

generate SCS-pincer complex **6** (Scheme 4, Figure 3).[44,45] When the same reaction was performed at room temperature, it

Scheme 4. Formation and Reactivity of SCS-Pincer Complex 6

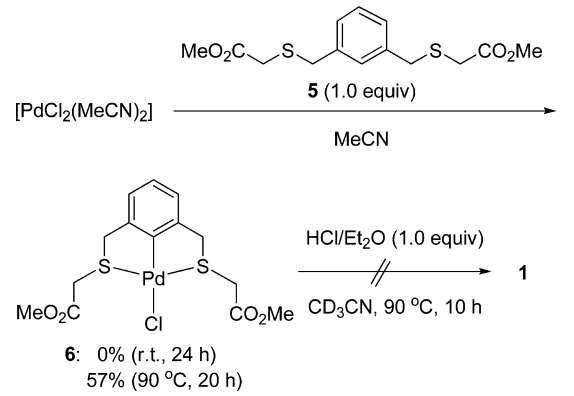

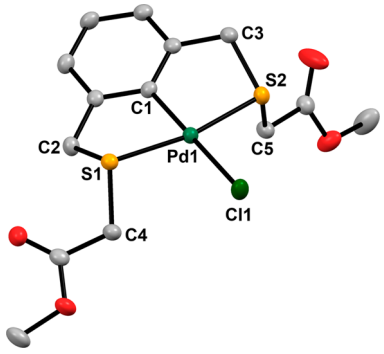

Figure 3. Molecular structure of **6**. Thermal ellipsoids are shown at a 50% probability level. Hydrogen atoms are omitted for clarity. Selected bond distances (Å), bond angles (deg), and dihedral angles (deg): Pd1–C1 = 1.980(2), Pd1–S1 = 2.2967(7), Pd1–S2 = 2.3151(7), Pd1–Cl1 = 2.3961(7), C1–Pd1–S1 = 83.11(6), C1–Pd1–S2 = 84.46(6), S1–Pd1–Cl1 = 96.27(3), S2–Pd1–Cl1 = 96.12(2), Pd1–S1–C2 = 99.24(7), Pd1–S1–C4 = 105.61(7), C2–S1–C4 = 104.64(10), Pd1–S2–C3 = 97.67(7), Pd1–S2–C5 = 102.18(7), C3–S2–C5 = 100.81(11), C1–Pd1–S1–C2 = 25.12(10), C1–Pd1–S2–C3 = 24.22(10), C1–Pd1–S1–C4 = 133.26(10), C1–Pd1–S2–C5 = 78.64(10).

produced an insoluble solid in nearly quantitative yield; the product appeared to be a monomer and/or oligomers of a 1:1 complex of $PdCl_2$ and **5**, according to the results of elemental analyses (Anal. Calcd for $C_{14}H_{18}Cl_2O_4PdS_2$: C, 34.19; H, 3.69. Found: C, 34.11; H, 3.56.).[45] Thus, the steric hindrance derived from the four methyl groups at the benzylic positions in **2** facilitates the aromatic C(sp^2)–H bond activation by placing the palladium atom proximate to the C(sp^2)–H bond at the 2-position. Even at 90 °C, **1** did not form from the mixtures of either $[PdCl_2(MeCN)_2]$ and **5** or **6** and HCl (Scheme 4).

A possible mechanism for the formation of complex **1** from $[PdCl_2(MeCN)_2]$ and **2** is shown in Scheme 5. After the

Scheme 5. Possible Mechanism for the Formation of 1 from $[PdCl_2(MeCN)_2]$ and 2

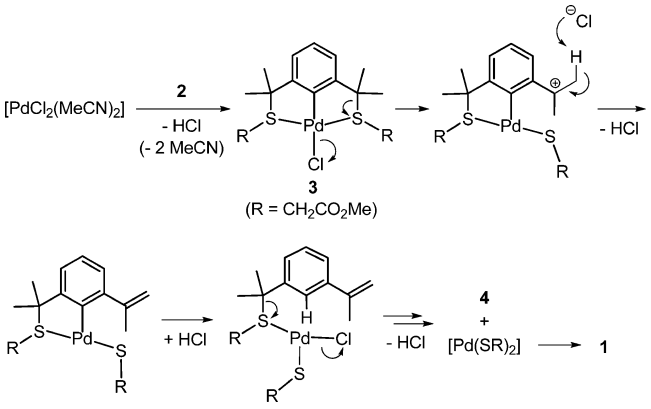

generation of SCS-pincer complex **3** via aromatic C(sp^2)–H bond activation, one of the thiolate groups is eliminated to provide a tertiary carbocation at the benzylic position with concurrent dissociation of a chloride ligand from palladium. This step rationalizes the difference in the reactivity of **3** and **6** because the generation of a carbocation intermediate from **6** is less favorable. Subsequent deprotonation affords a carbon–carbon double bond. The protonolysis of the aromatic C(sp^2)–Pd bond by HCl followed by E1 elimination similar to that described above occurs again to give **4** and a mononuclear palladium thiolate, $[Pd(SCH_2CO_2Me)_2]$, which then aggregates to construct a stable tiara-like octanuclear architecture. Although the above mechanism explains the formation of **1**, the bidentate coordination of **2** to $PdCl_2$ without aromatic C(sp^2)–H bond activation[45] and the subsequent stepwise elimination of the thiolate groups, similar to the above mechanism, can proceed concurrently to form **1**.

For examining whether a small amount of the hexanuclear complex $[Pd(\mu\text{-}SCH_2CO_2Me)_2]_6$ is formed through the conventional method (Scheme 1) or the alternative method (Scheme 2), the crude reaction mixtures were analyzed by MALDI-TOF MS. No peak assignable to $[Pd(\mu\text{-}SCH_2CO_2Me)_2]_6$ (with Na^+, calcd 1921.4) was detected. Both these methods afforded **1** selectively; therefore, the predominant formation of the octanuclear complex over a hexanuclear complex seems to result not from the reaction conditions but from the structure of the substituents on the sulfur atoms, that is, the methoxycarbonylmethyl groups, which can be regarded as a template. In the case of nickel, the aforementioned $[Ni(\mu\text{-}SCH_2CO_2Et)_2]_8$ is the sole example of an octanuclear tiara-like complex, reported by Dance et al.[18] They mentioned that the size of the tiara ring can be determined by the van der Waals volume of the ethoxycarbonylmethyl group, which, similar to that of **1**, also bends inward to occupy the inner void in the crystal structure. Dahl et al. proposed that macrocyclic $[Ni(\mu\text{-}SPh)_2]_{11}$ was constructed

dx.doi.org/10.1021/ic403050c | Inorg. Chem. 2014, 53, 3558–3567

around a THF molecule, which operated as a template during the growth of a ribbon-like nickel thiolate oligomer.[21] On the other hand, $[Pd(\mu\text{-}SCH_2CO_2Me)_2]_6$, which is a hexanuclear analogue of **1**, was prepared from $PdCl_4^{2-}$ and thioglycolic acid in MeOH.[39] In this reaction, we presume that the formation of the hexanuclear tiara ring with carboxylic acids as substituents occurred first, and ester condensation between the carboxylic acid moieties and MeOH followed.

Synthesis and Structure of Tiara-like Octanuclear Platinum Complex 7. The synthesis of tiara-like platinum complexes was first examined using $PtCl_2$/methyl thioglycolate/DIEA similar to the reaction conditions described in Scheme 1 (in MeOH, 0.4 M, 80 °C, 10 h). A tiara-like octanuclear complex, $[Pt(\mu\text{-}SCH_2CO_2Me)_2]_8$ (**7**), was formed in moderate yield (~60%); however, byproducts, which may contain tiara-like complexes with different-sized rings as speculated from the ^{1}H NMR analysis, were formed concurrently, and the isolation of **7** from the mixture was unsuccessful. MALDI-TOF MS analysis of the crude reaction mixture showed small peaks assignable to $[Pt(\mu\text{-}SCH_2CO_2Me)_2]_9$ at m/z 3673.3 (with Na^+, calcd 3671.2) and $[Pt(\mu\text{-}SCH_2CO_2Me)_2]_{10}$ at m/z 4075.4 (with Na^+, calcd 4076.5) in addition to a parent peak assignable to **7** at m/z 3267.7 (with Na^+, calcd 3264.7); no peaks corresponding to tiara-like complexes with smaller rings were detected. In contrast, when $PtCl_2$ was reacted with 1 equiv of **2** in MeCN (1 M) at 90 °C (bath temperature), **7** was obtained in high isolated yield with high purity (Scheme 6). The molecular

Scheme 6. Formation of Tiara-like Octanuclear Platinum Complex 7

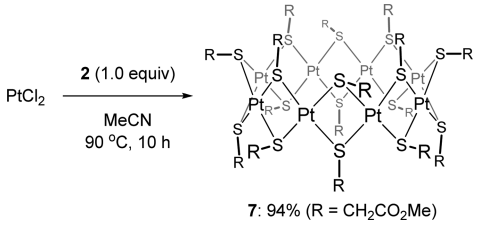

structure of **7** was also determined by X-ray crystallography (Figure 4, recrystallized from $CHCl_3$/octane). In contrast to **1**, the inside of the ring was void, and a solvent molecule ($CHCl_3$) was located outside the ring. The range of the distances between two adjacent platinum atoms is 3.2409(4)−3.3345(4) Å (average: 3.29(3) Å); these distances are slightly longer than those between two adjacent palladium atoms in **1**. The Pt−S bond distances range within 2.298(4)−2.356(6) Å (average: 2.32(1) Å) and are almost same as the Pd−S bond distances in **1**. The horizontal and vertical S−Pt−S bond angles vary within 94.88(19)−101.82(15)° (average: 98.4(16)°) and 79.42(14)−85.3(2)° (average: 81.8(12)°), respectively, while the Pt−S−Pt bond angles vary within 88.2(2)−92.33(7)° (average: 90.3(12)°). According to the comparison of the S−M−S and M−S−M bond angles in **1** and **7** (M = Pd and Pt, respectively), the tiara ring of **7** is more horizontally elongated than that of **1** as a result of the changes in these angles. The dihedral angles between the PtS_4 planes range within 129.93(13)−142.25(8)° (average: 135(4)°). The distances between two adjacent sulfur atoms in the two S_8 rings are within the range of 3.409(8)−3.615(6) Å (average: 3.51(4) Å) and are also slightly longer than those in **1**. The distances between the diagonally positioned platinum atoms are Pt1···Pt5 = 8.8011(5) Å, Pt2···Pt6 = 8.7539(5) Å, Pt3···Pt7 = 8.3559(5) Å, and Pt4···Pt8 = 8.4346(5) Å, resulting in an ellipsoidal architecture; the average distance (8.59 Å) is longer than that in **1** by ~0.15 Å.

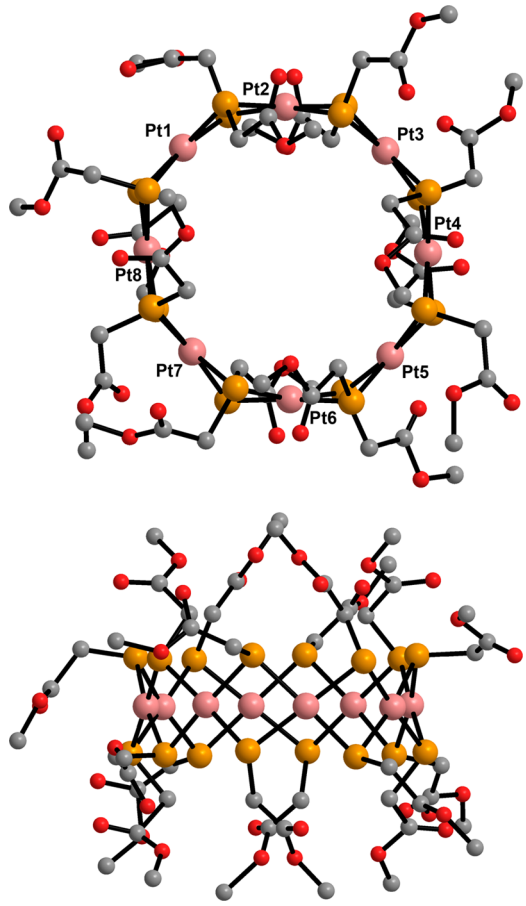

Figure 4. Molecular structure of **7**. (upper) Top view. (lower) Side view. A solvent molecule ($CHCl_3$) outside of the tiara ring and hydrogen atoms are omitted for clarity. Pt: pink, S: orange, C: gray, O: red.

The MALDI-TOF MS spectrum of isolated **7** reveals a parent peak at m/z 3265.7 as well as peaks at m/z 3191.7 and 3118.6 (Figures S4−S7 in Supporting Information), which are assigned to **7** with one or two methoxycarbonylmethyl group(s) missing, respectively (with Na^+, calcd 3190.7 and 3117.7). The ^{1}H NMR spectrum of **7** (in $CDCl_3$) reveals two methylene signals at 3.53 and 3.42 ppm and two methoxy signals at 3.96 and 3.76 ppm, which appeared in the same fashion as those in **1**. The variable-temperature measurements of **7** in $CDCl_3$ and CD_2Cl_2 indicated that the dynamic behavior of the axial arms was also similar to that observed in **1** (Figure 5), whereas no inward bend of the arms was observed in the crystal structure of **7**. Compared with **1**, the axial methoxy signal at 3.96 ppm was more broadened at low temperatures in $CDCl_3$. The HMBC spectrum of **7** measured in $CDCl_3$ also revealed correlations between carbonyl carbons (169.9 and 170.1 ppm), the axial methoxy protons (3.96 ppm), and methylene protons (3.53 ppm), as well as the equatorial methoxy protons (3.76 ppm) and other methylene protons (3.42 ppm); therefore, the singlet at 3.53 ppm is assignable to the methylene protons in the axial arms, and the other singlet at 3.42 ppm is assignable to the methylene protons in the equatorial arms. These observations indicate that the

dx.doi.org/10.1021/ic403050c | Inorg. Chem. 2014, 53, 3558−3567

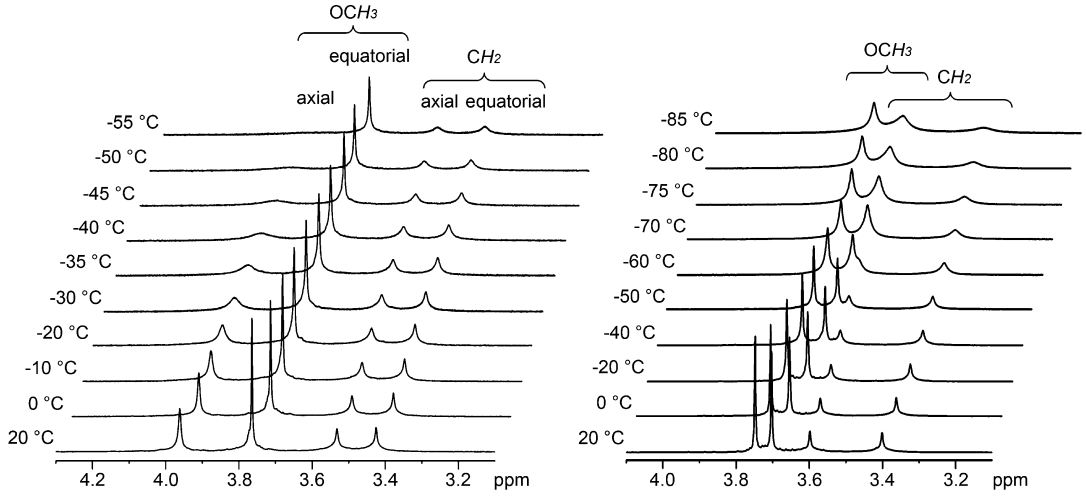

Figure 5. Variable-temperature ^{1}H NMR spectra (400 MHz) of **7** in (left) $CDCl_3$, −55−20 °C and (right) CD_2Cl_2, −85−20 °C.

methoxycarbonylmethyl groups should operate as a template during the formation of **7** in a manner similar to that of **1**.

A more dilute reaction (0.04 M) resulted in the formation of SCS-pincer complex **8** (15%) in addition to **7** (57%). After isolation, **8** was heated to 90 °C in CD_3CN (0.4 M) in the presence of 1 equiv of HCl; however, **7** did not form, thereby this reaction differs from the corresponding reaction involving palladium (Scheme 7). These results indicate that the formation of **7** does not proceed via SCS-pincer complex **8** but rather through monomeric and/or oligomeric 1:1 complexes of $PtCl_2$ and **2**. The plausible formation mechanism of **7** from the 1:1 complexes is analogous to the mechanism described for the palladium complex above.

Scheme 7. Reaction of SCS-Pincer Complex 8 with HCl

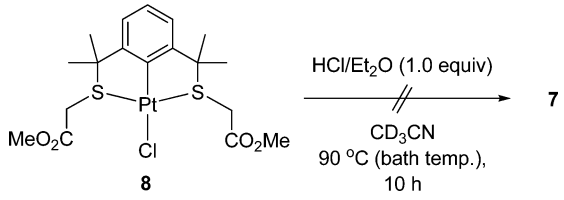

A trial for the formation of tiara-like palladium/platinum mixed complexes was performed through the reaction of **1** with **7** in CD_3CN at 70 °C. However, these complexes remained intact even after 48 h, and mixed complexes were not obtained, as confirmed by the ^{1}H NMR and MALDI-TOF MS measurements.

Inclusion Complexes with Dihalo- or Iodoalkanes. The diameters of the inner voids of **1** and **7** are ∼5.1−5.2 Å, taking into account the van der Waals radii of palladium (1.63 Å) and platinum (1.75 Å).[46] We found that the recrystallization of **1** and **7** from the mixtures of good solvents, such as CH_2Cl_2, $ClCH_2CH_2Cl$, CH_2Br_2, and CH_3I, and poor solvents, such as hexane and Et_2O, gave the corresponding inclusion complexes, that is, **1**·CH_2Cl_2, **1**·$ClCH_2CH_2Cl$, **1**·CH_2Br_2, **1**·CH_3I, **7**·CH_2Cl_2, **7**·$ClCH_2CH_2Cl$, and, **7**·CH_2Br_2, respectively. The top and side views of the molecular structures of these complexes are shown in Figures 6 and 7. The guest molecules are disordered in these inclusion complexes, except for that in **1**·CH_2Cl_2; only the configurations with highest occupancy are depicted. In **1**·CH_2Cl_2 and **1**·CH_2Br_2, one of the two C−X bonds (X = Cl, Br) is arranged vertically, and the other C−X bond is nearly horizontal. In contrast, in **7**·CH_2Cl_2 and **7**·CH_2Br_2, the guest molecules themselves are oriented more vertically. The $ClCH_2CH_2Cl$ molecules in **1**·$ClCH_2CH_2Cl$ and **7**·$ClCH_2CH_2Cl$ are also vertically oriented. In **1**·CH_3I, the CH_3I molecule maintains a relatively horizontal position. The distances between the diagonally positioned metal atoms, average distances, and oblateness values, which is defined as 1 − (short radius/long radius), are summarized in Table 1. The M1···M5 and M3···M7 distances correspond to the lengths of the major and minor axes of the ellipsoidal architectures,

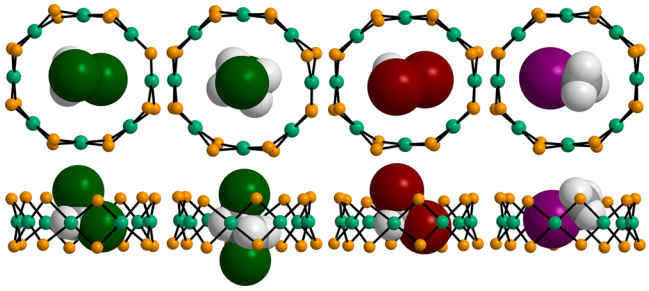

Figure 6. Molecular structures of **1**·CH_2Cl_2, **1**·$ClCH_2CH_2Cl$, **1**·CH_2Br_2, and **1**·CH_3I. (upper) Top views. (lower) Side views. Methoxycarbonylmethyl groups and solvent molecules outside of the tiara rings are omitted for clarity. The guest molecules are depicted in a space-filling model. Pd: light green, S: orange, Cl: green, Br: brown, I: purple, C: gray, H: white.

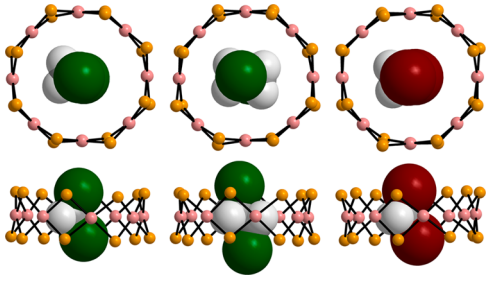

Figure 7. Molecular structures of **7**·CH_2Cl_2, **7**·$ClCH_2CH_2Cl$, and **7**·CH_2Br_2. (upper) Top views. (lower) Side views. Methoxycarbonylmethyl groups and solvent molecules outside of the tiara rings are omitted for clarity. The guest molecules are depicted in a space-filling model. Pt: pink, S: orange, Cl: green, Br: brown, C: gray, H: white.

dx.doi.org/10.1021/ic403050c | Inorg. Chem. 2014, 53, 3558−3567

Table 1. Diagonally Positioned Metal···Metal Distances (Å), Average Distances (Å), and Oblateness Values for 1, 7, and Their Inclusion Complexes

complex	M1···M5	M2···M6	M3···M7	M4···M8	average	oblateness
1	8.7191(9)	8.2331(9)	8.2307(8)	8.5895(8)	8.44	0.056
1·CH_2Cl_2	8.7614(9)	8.5509(9)	8.0743(9)	8.4117(9)	8.45	0.078
1·$ClCH_2CH_2Cl$	8.5720(19)	8.5711(15)	8.3447(18)	8.3465(16)	8.46	0.027
1·CH_2Br_2	8.7857(13)	8.4094(13)	8.0890(13)	8.5747(12)	8.46	0.079
1·CH_3I	8.7466(6)	8.4364(6)	8.1490(6)	8.5861(6)	8.48	0.068
7	8.8011(5)	8.7539(5)	8.3559(5)	8.4346(5)	8.59	0.051
7·CH_2Cl_2	8.7880(23)	8.6775(28)	8.3819(19)	8.5212(19)	8.59	0.046
7·$ClCH_2CH_2Cl$	8.7416(23)	8.7017(28)	8.3991(20)	8.5102(22)	8.59	0.039
7·CH_2Br_2	8.7935(23)	8.5500(20)	8.4057(20)	8.6355(29)	8.60	0.044

respectively. In the palladium complexes, the toroidal architecture flexes to accommodate the guest molecules, as is evident from the distances mentioned above (major axis: 8.57−8.79 Å and minor axis: 8.07−8.34 Å), which is similar to the behavior reported for $[Ni(\mu\text{-}StBu)(\mu\text{-mtet})]_{10}$ (mtet = 2-methylthioethanethiolate).[20] In contrast, the platinum complexes did not undergo any significant change in shape in the presence of the guest molecules (major and minor axes lengths of 8.74−8.79 Å and 8.38−8.41 Å, respectively). The oblateness also indicates the difference in the flexibilities of **1** and **7**. Among these complexes, the architecture of **1**·$ClCH_2CH_2Cl$ is the closest to a true circle, whereas **1**·CH_2Cl_2 and **1**·CH_2Br_2 have the most ellipsoidal structures.

As shown in Figure 8, the weak CH···Cl hydrogen bonds between the methylene protons of the four axially positioned

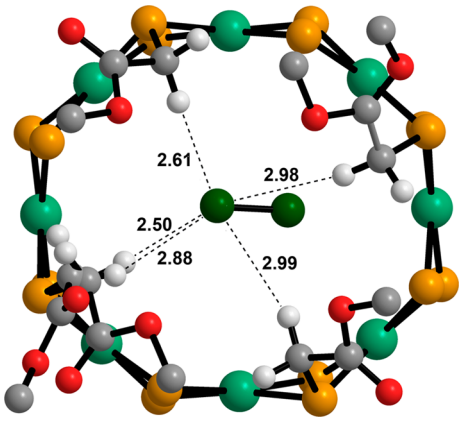

Figure 8. CH···Cl hydrogen bonds in **1**·CH_2Cl_2 (top view). Only the tiara ring, four axial methoxycarbonylmethyl groups (two disordered), and a CH_2Cl_2 molecule are shown. The numbers represent the H···Cl atomic distances (Å). Pd: light green, S: orange, Cl: green, C: gray, O: red, H: white.

methoxycarbonylmethyl groups and the chlorine atom of CH_2Cl_2 in **1**·CH_2Cl_2 stabilize the inclusion structure. The H···Cl atomic distances (2.50−2.99 Å) are typical for this type of hydrogen bonding.[47,48] Weak CH···X hydrogen bonds (X = Cl, Br) were observed not only in **1**·CH_2Cl_2 but also in other dihaloalkane inclusion complexes. The ranges of the corresponding atomic distances and average distances are summarized in Table 2. The shortest distances between the halogen atoms of the guest molecules and palladium atoms in **1**·CH_2Cl_2 (3.249(5) Å), **1**·CH_2Br_2 (3.187(3) Å), and **1**·CH_3I (3.3214(10) Å) are slightly shorter than the sum of the van der Waals radii of palladium (1.63 Å) and the corresponding halogen atoms (Cl: 1.75 Å, Br: 1.85 Å, I: 1.98 Å) by ∼0.1, 0.3, and 0.3 Å, respectively; this indicates weak coordination of the halogen atoms to the palladium atoms.

Table 2. Ranges of CH···X Distances (X = Cl, Br) (Å) and Average Distances (Å) in **1**·CH_2Cl_2, **1**·$ClCH_2CH_2Cl$, **1**·CH_2Br_2, **7**·CH_2Cl_2, **7**·$ClCH_2CH_2Cl$, and **7**·CH_2Br_2

complex	range of CH···X distances	average
1·CH_2Cl_2	2.50−2.99	2.79(22)
1·$ClCH_2CH_2Cl$	2.69−3.01	2.87(9)
1·CH_2Br_2	2.47−3.18	2.8(4)
7·CH_2Cl_2	2.55−3.19	2.93(18)
7·$ClCH_2CH_2Cl$	2.70−2.96	2.83(9)
7·CH_2Br_2	2.86−3.18	2.98(11)

CONCLUSION

We synthesized a tiara-like octanuclear palladium complex via a conventional method, which involved a thiol and base, and via an alternative method using dimethyl [1,3-phenylenebis(1-methylethylidenethio)]diacetate. In the latter method, the resultant tiara-like complex formed via the corresponding SCS−pincer complex and/or 1:1 complexes of $PdCl_2$ and the ligand. The alternative method is effective for the synthesis of a highly pure tiara-like octanuclear platinum complex. Both of these tiara-like complexes had an ellipsoidal architecture; the platinum tiara ring was more horizontally elongated than the palladium tiara ring because of the differences in the S−M−S and M−S−M bond angles, whereas the M−S bond distances were almost equivalent in the palladium and platinum complexes. In $CDCl_3$, these complexes showed the dynamic behaviors in which the axial arms would move into and out of the tiara ring, whereas no such behaviors were observed in CD_2Cl_2. The inclusion of dihalo- or iodoalkanes into the tiara-like complexes was also successful. The toroidal architecture flexed to accommodate the guest molecules in the palladium inclusion complexes, whereas no significant change in the shape occurred upon the inclusion of guest molecules in the platinum inclusion complexes. Weak CH···X hydrogen bonding (X = Cl, Br) as well as weak coordination of the halogen atoms to palladium atoms stabilize these inclusion structures. Other small molecules would also be expected to be accommodated in the inner void of the tiara rings, and some of them may have much stronger interactions with transition-metal atoms, resulting in a unique behavior and reactivity.

EXPERIMENTAL SECTION

Materials and Methods. All manipulations were performed under an argon atmosphere using standard Schlenk techniques. Dry solvents were purchased from either Wako Chemical or Nacalai. Flash column

dx.doi.org/10.1021/ic403050c | Inorg. Chem. 2014, 53, 3558−3567

chromatography was performed using silica gel SiliCycle SiliaFlash F60 (40−63 μm, 230−400 mesh).

Physical and Analytical Measurements. NMR spectra were recorded on either a JEOL AL-400 (400 MHz (^{1}H), 100 MHz (^{13}C), 85.7 MHz (^{195}Pt)) or a Bruker AV-300N (300 MHz (^{1}H), 75 MHz (^{13}C)) spectrometer. Chemical shift values (δ) in ^{1}H and ^{13}C NMR spectra were expressed relative to $SiMe_4$. ^{195}Pt NMR spectra were referenced using an external reference (0.3 M K_2PtCl_4 in D_2O, δ = −1628 ppm). Infrared (IR) measurements were carried out using a JASCO FT/IR-6100 spectrometer. Elemental analysis was obtained using a J-Science Lab JM-10 analyzer. MALDI-TOF MS spectra were recorded on a Shimadzu Axima Performance spectrometer. Melting points were measured on a Yanagimoto micro melting point apparatus.

Synthesis of [Pd(μ-SCH$_2$CO$_2$Me)$_2$]$_8$ (1). To a mixture of methyl thioglycolate (51 μL, 0.57 mmol), DIEA (96 μL, 0.56 mmol), and *n*-propanol (0.95 mL), $PdCl_2$ (50 mg, 0.28 mmol) was added, and the reaction mixture was stirred at room temperature for 4 h. After filtration, the orange-yellow solid was dried under vacuum and obtained in 90% isolated yield (81 mg, 0.032 mmol). Recrystallization from $CHCl_3$/hexane gave yellow block crystals. ^{1}H NMR (400 MHz, $CDCl_3$) δ 3.97 (s, 24H, *ax*-CO_2CH_3), 3.77 (s, 24H, *eq*-CO_2CH_3), 3.34 (s, 16H, *ax*-CH_2), 3.23 (s, 16H, *eq*-CH_2). ^{1}H NMR (400 MHz, CD_2Cl_2) δ 3.75 (s, 24H, CO_2CH_3), 3.72 (s, 24H, CO_2CH_3), 3.38 (s, 16H, CH_2), 3.22 (s, 16H, CH_2). ^{13}C NMR (75 MHz, $CDCl_3$) δ 170.4 (*ax*-CO_2Me), 169.8 (*eq*-CO_2Me), 53.1 (*ax*-CO_2CH_3), 52.7 (*eq*-CO_2CH_3), 35.6 (*eq*-CH_2), 30.6 (*ax*-CH_2). IR (ν_{CO}, KBr): 1735 cm^{-1}. Mp 143−144 °C (dec.). Anal. Calcd for $C_{48}H_{80}O_{32}Pd_8S_{16}$: C, 22.76; H, 3.18. Found: C, 22.65; H, 3.02.

Synthesis of Dimethyl [1,3-Phenylenebis(1-methylethylidenethio)]diacetate (2). Compound **2** was prepared by reference to a reported synthetic procedure for similar compounds.[49] To a mixture of α,α′-dihydroxy-1,3-diisopropylbenzene (776 mg, 3.99 mmol), ZnI_2 (1.28 g, 4.01 mmol), and methyl thioglycolate (0.750 mL, 8.39 mmol), dry 1,2-dichloroethane (25 mL) was added, and the reaction mixture was stirred at room temperature for 1 h. The mixture was diluted with dichloromethane and washed with water. The organic layer was then washed with 1 M NaOH and dried over $MgSO_4$. After filtration and removal of the solvents, the residue was purified by silica gel column chromatography (eluent: hexane/ethyl acetate = 3:1) to give **2** (1.42 g, 3.82 mmol) in 96% isolated yield as a colorless oil. ^{1}H NMR (300 MHz, $CDCl_3$) δ 7.71 (t, J = 1.5 Hz, 1H, Ar-2-*H*), 7.37 (dd, J = 6.6, 1.5 Hz, 2H, Ar-4,6-*H*), 7.28 (t, J = 6.9 Hz, 1H, Ar-5-*H*), 3.59 (s, 6H, CO_2CH_3), 2.98 (s, 4H, CH_2), 1.73 (s, 12H, CH_3). ^{13}C NMR (75 MHz, $CDCl_3$) δ 171.0 (CO_2Me), 145.2 (Ar-1,3), 127.9 (Ar-5), 125.1 (Ar-4,6), 125.0 (Ar-2), 52.3 (CO_2CH_3), 48.6 ($C(CH_3)_2$), 32.1 (SCH_2), 29.9 ($C(CH_3)_2$).

Alternative Synthesis of Complex 1. To a mixture of [$PdCl_2$(MeCN)$_2$] (78 mg, 0.30 mmol) and **2** (112 mg, 0.30 mmol), dry methanol (1.0 mL) was added, and the reaction mixture was heated at 70 °C (bath temperature) for 10 h. After filtration, the orange-yellow precipitate was dried under vacuum and obtained in 84% isolated yield (80 mg, 0.031 mmol). Recrystallization from $CHCl_3$/hexane gave yellow block crystals.

Synthesis of SCS-Pincer Palladium Complex 3. To a mixture of [$PdCl_2$(MeCN)$_2$] (1.00 g, 3.86 mmol) and **2** (1.43 g, 3.86 mmol), dry chloroform (100 mL) was added, and the reaction mixture was stirred at room temperature for 1 h. The obtained crude compound was purified by silica gel column chromatography (eluent: hexane/ethyl acetate = 1:2) to give **3** as a pale orange-yellow solid (1.64 g, 3.20 mmol) in 83% isolated yield. ^{1}H NMR (300 MHz, $CDCl_3$) δ 7.11 (t, J = 7.8 Hz, 1H, Ar-4-*H*), 6.80 (d, J = 7.5 Hz, 2H, Ar-3,5-*H*), 4.50−3.85 (br, 4H, CH_2), 3.76 (s, 6H, CO_2CH_3), 1.81 (s, 12H, CH_3). ^{13}C NMR (100 MHz, $CDCl_3$) δ 167.1 (CO_2Me), 154.1 (Ar-2,6), 152.7 (br, Ar-1), 125.0 (Ar-4), 123.1 (Ar-3,5), 63.4 ($C(CH_3)_2$), 52.3 (CO_2CH_3), 35.7 (SCH_2), 31.1 (br, CH_3), 29.4 (br, CH_3). IR (ν_{CO}, KBr): 1739 cm^{-1}. Mp 119−121 °C (dec.). Anal. Calcd for $C_{18}H_{25}ClO_4PdS_2$: C, 42.28; H, 4.93. Found: C, 42.31; H, 4.85.

Synthesis of Dimethyl [1,3-Phenylenebis(methylenethio)]-diacetate (5). To a mixture of methyl thioglycolate (240 μL, 2.68 mmol) and DIEA (455 μL, 2.68 mmol), dry methanol (10 mL) was added, and the reaction mixture was stirred at room temperature for 15 min. α,α′-Dibromo-*m*-xylene (335 mg, 1.27 mmol) was then added, and the mixture was stirred at 70 °C for 10 h. After drying under vacuum, the obtained crude compound was purified by silica gel column chromatography (eluent: hexane/ethyl acetate = 3:1) to give **5** (392 mg, 1.25 mmol) in 98% isolated yield as a colorless oil. ^{1}H NMR (300 MHz, $CDCl_3$) δ 7.31−7.21 (m, 4H, Ar-2,4,5,6-*H*), 3.81 (s, 4H, ArCH_2), 3.72 (s, 6H, CO_2CH_3), 3.08 (s, 4H, CH_2CO_2Me). ^{13}C NMR (75 MHz, $CDCl_3$) δ 170.5 (CO_2Me), 137.3 (Ar-1,3), 129.6 (Ar-5), 128.5 (Ar-2), 127.9 (Ar-4,6), 52.1 (CO_2CH_3), 35.9 (ArCH_2), 31.8 (CH_2CO_2Me).

Synthesis of SCS-Pincer Palladium Complex 6. To a mixture of [$PdCl_2$(MeCN)$_2$] (15 mg, 0.059 mmol) and **5** (19 mg, 0.060 mmol), dry acetonitrile (1.5 mL) was added, and the reaction mixture was stirred at 90 °C (bath temperature) for 20 h. The pale yellow solution was vacuumed to dry. Reprecipitation from $CHCl_3$/hexane gave a pale yellow solid (15 mg, 0.033 mmol) in 57% isolated yield. Recrystallization from $CHCl_3$/hexane gave pale yellow block crystals. ^{1}H NMR (300 MHz, $CDCl_3$) δ 7.04−6.94 (m, 3H, Ar-3,4,5-*H*), 4.60−3.90 (br, 8H, CH_2), 3.79 (s, 6H, CO_2CH_3). ^{13}C NMR (100 MHz, $CDCl_3$) δ 167.6 (CO_2Me), 158.5 (br, Ar-1), 147.6 (br, Ar-2,6), 125.2 (Ar-4), 122.7 (Ar-3,5), 53.1 (CO_2CH_3), 48.5 (br, ArCH_2), 39.9 (br, CH_2CO_2Me). IR (ν_{CO}, KBr): 1734 cm^{-1}. Mp 112−113 °C (dec). Anal. Calcd for $C_{14}H_{17}ClO_4PdS_2$: C, 36.93; H, 3.76. Found: C, 36.58; H, 3.99.

Synthesis of [Pt(μ-SCH$_2$CO$_2$Me)$_2$]$_8$ (7). To a mixture of $PtCl_2$ (662 mg, 2.49 mmol) and **2** (922 mg, 2.49 mmol), dry acetonitrile (1.25 mL) was added, and the reaction mixture was stirred at 90 °C (bath temperature) for 10 h. The yellow solution was evaporated under vacuum to dry. Recrystallization from $CHCl_3$/heptane gave yellow block crystals (950 mg, 0.293 mmol) in 94% isolated yield. ^{1}H NMR (400 MHz, $CDCl_3$) δ 3.96 (s, 24H, *ax*-CO_2CH_3), 3.76 (s, 24H, *eq*-CO_2CH_3), 3.53 (s, 16H, *ax*-CH_2), 3.42 (s, 16H, *eq*-CH_2). ^{1}H NMR (400 MHz, CD_2Cl_2) δ 3.75 (s, 24H, CO_2CH_3), 3.70 (s, 24H, CO_2CH_3), 3.60 (s, 16H, CH_2), 3.40 (s, 16H, CH_2). ^{13}C NMR (75 MHz, $CDCl_3$) δ 170.1 (*eq*-CO_2Me), 169.9 (*ax*-CO_2Me), 52.9 (*ax*-CO_2CH_3), 52.6 (*eq*-CO_2CH_3), 37.1 (*eq*-CH_2), 30.2 (*ax*-CH_2). ^{195}Pt NMR (85.7 MHz, $CDCl_3$) δ −3247.3 (br). IR (ν_{CO}, KBr): 1733 cm^{-1}. Mp 178−180 °C (dec). Anal. Calcd for $C_{48}H_{80}O_{32}Pt_8S_{16}$: C, 17.78; H, 2.49. Found: C, 18.11; H, 2.55.

SCS-Pincer Platinum Complex 8. To a mixture of $PtCl_2$ (369 mg, 1.39 mmol) and **2** (513 mg, 1.39 mmol), dry acetonitrile (36 mL) was added, and the reaction mixture was stirred at 90 °C (bath temperature) for 20 h. The yellow solution was evaporated under vacuum to dry. The resulting yellow oil was dissolved in $CHCl_3$, and hexane was poured into the solution to remove **7**. After filtration, the filtrate was dried under vacuum, and the obtained crude compound was purified by silica gel column chromatography (eluent: hexane/ethyl acetate = 1:1) to give **8** (124 mg, 0.206 mmol) in 15% isolated yield as a pale yellow solid. ^{1}H NMR (300 MHz, CD_3CN) δ 7.13 (t, J = 7.8 Hz, 1H, Ar-4-*H*), 6.86 (d, J = 7.5 Hz, 2H, Ar-3,5-*H*), 4.08−3.73 (m, 4H, CH_2), 3.67 (s, 6H, CO_2CH_3), 1.75 (s, 12H, CH_3). ^{13}C NMR (100 MHz, CD_3CN) δ 168.3 (t, $^3J_{C-Pt}$ = 23.8 Hz, CO_2Me), 153.8 (t, $^2J_{C-Pt}$ = 28.8 Hz, Ar-2,6), 145.1 (Ar-1), 144.6 (Ar-1), 125.4 (Ar-4), 123.8 (t, $^3J_{C-Pt}$ = 23.2 Hz, Ar-3,5), 67.8 (t, $^2J_{C-Pt}$ = 18.7 Hz, $C(CH_3)_2$), 53.4 (CO_2CH_3), 38.6 (SCH_2), 37.9 (SCH_2), 32.0 (CH_3), 31.3 (CH_3), 29.4 (CH_3), 28.6 (CH_3). ^{195}Pt NMR (85.7 MHz, CD_3CN) δ −4026.5 (quintet, $^3J_{Pt-H}$ = 42 Hz), −4028.2 (quintet, $^3J_{Pt-H}$ = 38 Hz). IR (ν_{CO}, KBr): 1736 cm^{-1}. Mp 131.5−132.5 °C (dec). Anal. Calcd for $C_{18}H_{25}ClO_4PdS_2$: C, 36.03; H, 4.20. Found: C, 36.11; H, 4.11.

Crystallographic Study of Complexes 1, 6, 7, 1·CH$_2$Cl$_2$, 1·ClCH$_2$CH$_2$Cl, 1·CH$_2$Br$_2$, 1·CH$_3$I, 7·CH$_2$Cl$_2$, 7·ClCH$_2$CH$_2$Cl, and 7·CH$_2$Br$_2$. Crystals suitable for X-ray diffraction measurements were obtained by recrystallization from $CHCl_3$/hexane for **1** (yellow block crystals), CH_2Cl_2/hexane for **6** (pale yellow block crystals), $CHCl_3$/octane for **7** (yellow block crystals), CH_2Cl_2/Et_2O for **1**·CH_2Cl_2 (yellow prism crystals), $ClCH_2CH_2Cl$/hexane for **1**·$ClCH_2CH_2Cl$ (yellow rod crystals), CH_2Br_2/hexane for **1**·CH_2Br_2 (yellow rod crystals), CH_3I/Et_2O for **1**·CH_3I (yellow block crystals), CH_2Cl_2/hexane for **7**·CH_2Cl_2 (yellow block crystals), $ClCH_2CH_2Cl$/Et_2O for

dx.doi.org/10.1021/ic403050c | Inorg. Chem. 2014, 53, 3558−3567

7·$ClCH_2CH_2Cl$ (yellow block crystals), and CH_2Br_2/hexane for 7·CH_2Br_2 (yellow cube crystals). The crystals dipped in liquid paraffin were mounted using a cryoloop and frozen at either 153 or 123 K. The diffraction data were collected with a Rigaku Saturn CCD detector (Mo Kα, λ = 0.71073 Å). Crystal data and structure refinement parameters are listed in Tables S1−S3 in Supporting Information. The structures were solved by direct methods using either SHELXS-2013[50] (for **1**, **1**·CH_2Cl_2, **1**·$ClCH_2CH_2Cl$, **1**·CH_2Br_2, and **1**·CH_3I), SHELXS-97[51] (for **6**), or SIR97[52] (for **7**, 7·CH_2Cl_2, 7·$ClCH_2CH_2Cl$, and 7·CH_2Br_2) and refined by least-squares on F^2, SHELXL-2013, or SHELXL-97 (for **6**).[50,51,53] Non-hydrogen atoms were anisotropically refined except for the disordered ones. Because methoxycarbonylmethyl groups and small organic molecules were disordered occasionally, bond distances in these moieties were restrained to be equal using a SADI command in SHELXL. All hydrogen atoms were placed at calculated positions. Refinements were continued until all shifts were smaller than one-tenth of the standard deviations of the parameters involved. Atomic scattering factors and anomalous dispersion terms were taken from the International Tables for X-ray Crystallography.[54]

MALDI-TOF MS Analysis of Tiara-like Complexes 1 and 7. Acetonitrile solutions of the tiara-like complexes (0.5 μL; **1**, 9.9 mM and **7**, 7.9 mM) were mixed with a H_2O/ethanol (1:1) solution of *trans*-retinoic acid (0.5 μL, 50.0 mM) and aqueous trifluoroacetic acid (aq TFA) (0.5 μL, 0.1%) on a MALDI plate and were analyzed. Calibration was performed using bradykinin fragment 1−7 in 0.1% aq TFA (10 μM), adrenocorticotropic hormone (ACTH) fragment 18−39 (human) in 0.1% aq TFA (10 μM), and α-cyano-4-hydroxycinnamic acid (4-CHCA).

■ ASSOCIATED CONTENT

Ⓢ Supporting Information

NMR spectra for new compounds, MALDI-TOF MS spectra for **1** and **7**, crystal data and structure refinement parameters for **1**, **6**, **7**, **1**·CH_2Cl_2, **1**·$ClCH_2CH_2Cl$, **1**·CH_2Br_2, **1**·CH_3I, 7·CH_2Cl_2, 7·$ClCH_2CH_2Cl$, and **7**·CH_2Br_2, and CIF files for **1**, **6**, **7**, **1**·CH_2Cl_2, **1**·$ClCH_2CH_2Cl$, **1**·CH_2Br_2, **1**·CH_3I, 7·CH_2Cl_2, 7·$ClCH_2CH_2Cl$, and 7·CH_2Br_2. CCDC reference numbers 974025 (**1**), 974026 (**6**), 974027 (**7**), 974058 (**1**·CH_2Cl_2), 974059 (**1**·$ClCH_2CH_2Cl$), 974060 (**1**·CH_2Br_2), 976482 (**1**·CH_3I), 976483 (7·CH_2Cl_2), 976484 (7·$ClCH_2CH_2Cl$), and 976485 (7·CH_2Br_2). This material is available free of charge via the Internet at http://pubs.acs.org.

■ AUTHOR INFORMATION

Corresponding Author

*E-mail: ura@cc.nara-wu.ac.jp.

Notes

The authors declare no competing financial interest.

■ ACKNOWLEDGMENTS

This work was partly supported by Grant-in-Aid for Scientific Research on Innovative Areas (Molecular Activation Directed toward Straightforward Synthesis) from The Ministry of Education, Culture, Sports, Science and Technology (MEXT), Japan. We thank Prof. Takashi Kajiwara (Nara Women's University) for supporting our X-ray crystallography.

■ REFERENCES

(1) Blower, P. J.; Dilworth, J. R. *Coord. Chem. Rev.* **1987**, *76*, 121.
(2) Jain, V. K.; Jain, L. *Coord. Chem. Rev.* **2010**, *254*, 2848.
(3) Mezei, G.; Zaleski, C. M.; Pecoraro, V. L. *Chem. Rev.* **2007**, *107*, 4933.
(4) Henkel, G.; Krebs, B. *Chem. Rev.* **2004**, *104*, 801.
(5) Lee, S. C.; Holm, R. H. *Chem. Rev.* **2004**, *104*, 1135.
(6) Ulman, A. *Chem. Rev.* **1996**, *96*, 1533.
(7) Whetten, R. L.; Shafigullin, M. N.; Khoury, J. T.; Schaaff, T. G.; Vezmar, I.; Alvarez, M. M.; Wilkinson, A. *Acc. Chem. Res.* **1999**, *32*, 397.
(8) Ananikov, V. P.; Beletskaya, I. P. *Dalton Trans.* **2011**, *40*, 4011.
(9) Ananikov, V. P.; Orlov, N. V.; Zalesskiy, S. S.; Beletskaya, I. P.; Khrustalev, V. N.; Morokuma, K.; Musaev, D. G. *J. Am. Chem. Soc.* **2012**, *134*, 6637.
(10) Ananikov, V. P.; Gayduk, K. A.; Beletskaya, I. P.; Khrustalev, V. N.; Antipin, M. Y. *Eur. J. Inorg. Chem.* **2009**, *2009*, 1149.
(11) Beletskaya, I. P.; Ananikov, V. P. *Eur. J. Org. Chem.* **2007**, *2007*, 3431.
(12) Ananikov, V. P.; Orlov, N. V.; Beletskaya, I. P.; Khrustalev, V. N.; Antipin, M. Y.; Timofeeva, T. V. *J. Am. Chem. Soc.* **2007**, *129*, 7252.
(13) Ananikov, V. P.; Orlov, N. V.; Beletskaya, I. P. *Organometallics* **2006**, *25*, 1970.
(14) Yang, Z.; Smetana, A. B.; Sorensen, C. M.; Klabunde, K. J. *Inorg. Chem.* **2007**, *46*, 2427.
(15) Zhang, C.; Matsumoto, T.; Samoc, M.; Petrie, S.; Meng, S.; Christopher Corkery, T.; Stranger, R.; Zhang, J.; Humphrey, M. G.; Tatsumi, K. *Angew. Chem., Int. Ed.* **2010**, *49*, 4209.
(16) Zhang, W.; Hong, J.; Zheng, J.; Huang, Z.; Zhou, J.; Xu, R. *J. Am. Chem. Soc.* **2011**, *133*, 20680.
(17) Kagalwala, H. N.; Gottlieb, E.; Li, G.; Li, T.; Jin, R.; Bernhard, S. *Inorg. Chem.* **2013**, *52*, 9094.
(18) Dance, I. G.; Scudder, M. L.; Secomb, R. *Inorg. Chem.* **1985**, *24*, 1201.
(19) Higgins, J. D., III; Suggs, J. W. *Inorg. Chim. Acta* **1988**, *145*, 247.
(20) Zhang, C.; Takada, S.; Kölzer, M.; Matsumoto, T.; Tatsumi, K. *Angew. Chem., Int. Ed.* **2006**, *45*, 3768.
(21) Ivanov, S. A.; Kozee, M. A.; Alex Merrill, W.; Agarwal, S.; Dahl, L. F. *J. Chem. Soc., Dalton Trans.* **2002**, 4105.
(22) Woodward, P.; Dahl, L. F.; Abel, E. W.; Crosse, B. C. *J. Am. Chem. Soc.* **1965**, *87*, 5251.
(23) Tan, C.; Jin, M.; Ma, X.; Zhu, Q.; Huang, Y.; Wang, Y.; Hu, S.; Sheng, T.; Wu, X. *Dalton Trans.* **2012**, *41*, 8472.
(24) Abel, E. W.; Crosse, B. C. *J. Chem. Soc. A* **1966**, 1377.
(25) Gould, R. O.; Harding, M. M. *J. Chem. Soc. A* **1970**, 875.
(26) Wark, T. A.; Stephan, D. W. *Organometallics* **1989**, *8*, 2836.
(27) Krüger, T.; Krebs, B.; Henkel, G. *Angew. Chem., Int. Ed. Engl.* **1989**, *28*, 61.
(28) Gaete, W.; Ros, J.; Solans, X.; Font-Altaba, M.; Brianso, J. L. *Inorg. Chem.* **1984**, *23*, 39.
(29) Jian, F.-F.; Jiao, K.; Li, Y.; Zhao, P.-S.; Lu, L.-D. *Angew. Chem., Int. Ed.* **2003**, *42*, 5722.
(30) Mahmoudkhani, A. H.; Langer, V. *Inorg. Chim. Acta* **1999**, *294*, 83.
(31) Koo, B.-K.; Block, E.; Kang, H.; Liu, S.; Zubieta, J. *Polyhedron* **1988**, *7*, 1397.
(32) Mahmoudkhani, A. H.; Langer, V. *Polyhedron* **1999**, *18*, 3407.
(33) Capdevila, M.; González-Duarte, P.; Sola, J.; Foces-Foces, C.; Cano, F. H.; Martínez-Ripoll, M. *Polyhedron* **1989**, *8*, 1253.
(34) Miyamae, H.; Yamamura, T. *Acta Crystallogr., Sect. C: Cryst. Struct. Commun.* **1988**, *44*, 606.
(35) Barrera, H.; Bayón, J. C.; Suades, J.; Germain, C.; Declerq, J. P. *Polyhedron* **1984**, *3*, 969.
(36) Kunchur, N. R. *Acta Crystallogr., Sect. B* **1968**, *B24*, 1623.
(37) Chui, S. S.-Y.; Low, K.-H.; Lu, J.; Roy, V. A. L.; Chan, S. L.-F.; Che, C.-M. *Chem.—Asian J.* **2010**, *5*, 2062.
(38) Stash, A.; Levashova, V.; Lebedev, S.; Hoskov, Y.; Mal'kov, A.; Romm, I. *Russ. J. Coord. Chem.* **2009**, *35*, 136.
(39) Schneider, I.; Horner, M.; Olendzki, R. N.; Strahle, J. *Acta Crystallogr., Sect. C: Cryst. Struct. Commun.* **1993**, *49*, 2091.
(40) Stash, A. I.; Perepelkova, T. I.; Noskov, Y. G.; Buslaeva, T. M.; Romm, I. P. *Russ. J. Coord. Chem.* **2001**, *27*, 585.
(41) Kumbhare, L. B.; Wadawale, A. P.; Jain, V. K.; Kolay, S.; Nethaji, M. *J. Organomet. Chem.* **2009**, *694*, 3892.
(42) Kumbhare, L. B.; Jain, V. K.; Phadnis, P. P.; Nethaji, M. *J. Organomet. Chem.* **2007**, *692*, 1546.

(43) Dey, S.; Jain, V. K.; Klein, A.; Kaim, W. *Inorg. Chem. Commun.* **2004**, *7*, 601.
(44) Lucena, N.; Casabó, J.; Escriche, L.; Sánchez-Castelló, G.; Teixidor, F.; Kivekäs, R.; Sillanpää, R. *Polyhedron* **1996**, *15*, 3009.
(45) Bergbreiter, D. E.; Osburn, P. L.; Liu, Y.-S. *J. Am. Chem. Soc.* **1999**, *121*, 9531.
(46) Bondi, A. *J. Phys. Chem.* **1964**, *68*, 441.
(47) Steiner, T. *Acta Crystallogr.* **1998**, *54*, 456.
(48) Hartmann, M.; Wetmore, S. D.; Radom, L. *J. Phys. Chem. A* **2001**, *105*, 4470.
(49) Kulkarni, V.; Cohen, T. *Tetrahedron* **1997**, *53*, 12089.
(50) Sheldrick, G. M. *SHELXL-2013;* University of Göttingen: Gottingen, Germany, 2013.
(51) Sheldrick, G. M. *SHELXTL-PC Package;* Bruker AXS, Inc.: Madison, WI, 1998.
(52) Altomare, A.; Burla, M. C.; Camalli, M.; Cascarano, G. L.; Giacovazzo, C.; Guagliardi, A.; Moliterni, A. G. G.; Polidori, G.; Spagna, R. *J. Appl. Crystallogr.* **1999**, *32*, 115.
(53) Sheldrick, G. M. *Acta Crystallogr.* **2008**, *A64*, 112.
(54) *International Tables for X-ray Crystallography;* Ibers, J. A., Hamilton, W. C., Eds.; Kynoch Press: Birmingham, UK, 1974; Vol. *IV*.

dx.doi.org/10.1021/ic403050c | *Inorg. Chem.* 2014, 53, 3558−3567